PHYSICAL REVIEW D **87,** 074010 (2013)

Anomalous enhancement observed in $B \to D^{(*)}\tau\bar{\nu}_\tau$ decays

P. Biancofiore,[1,2] P. Colangelo,[2] and F. De Fazio[2]

[1]*Dipartimento di Fisica, Università di Bari, via Orabona 4, 70126 Bari, Italy*

[2]*Istituto Nazionale di Fisica Nucleare, Sezione di Bari, via Orabona 4, 70126 Bari, Italy*

(Received 11 February 2013; published 11 April 2013)

The *BABAR* measurements of the ratios $\mathcal{R}(D^{(*)}) = \frac{\mathcal{B}(B\to D^{(*)}\tau\bar{\nu}_\tau)}{\mathcal{B}(B\to D^{(*)}\mu\bar{\nu}_\mu)}$ deviate from the standard model expectation, while new results on the purely leptonic $B \to \tau\bar{\nu}_\tau$ mode show a better consistency with the standard model, within the uncertainties. In a new physics scenario, one possibility to accommodate these two experimental facts consists in considering an additional tensor operator in the effective weak Hamiltonian. We study the effects of such an operator in a set of observables, in semileptonic $B \to D^{(*)}$ modes as well as in semileptonic B and B_s decays to excited positive-parity charmed mesons.

DOI: 10.1103/PhysRevD.87.074010 PACS numbers: 13.20.He, 12.60.−i

I. INTRODUCTION

The *BABAR* measurements of the rates of B^- and $\bar{B}^0$ semileptonic decays into $D^{(*)}$ and a τ lepton seem to indicate a significant deviation from the standard model (SM) expectation. The experimental results concern the $B \to D^{(*)}\tau\bar{\nu}_\tau$ decay widths normalized to the widths of the corresponding modes having a light $\ell = e$, μ lepton in the final state [1]:

$$\begin{aligned}
\mathcal{R}^-(D) &= \frac{\mathcal{B}(B^- \to D^0\tau^-\bar{\nu}_\tau)}{\mathcal{B}(B^- \to D^0\ell^-\bar{\nu}_\ell)} = 0.429 \pm 0.082 \pm 0.052,\\
\mathcal{R}^-(D^*) &= \frac{\mathcal{B}(B^- \to D^{*0}\tau^-\bar{\nu}_\tau)}{\mathcal{B}(B^- \to D^{*0}\ell^-\bar{\nu}_\ell)} = 0.322 \pm 0.032 \pm 0.022,\\
\mathcal{R}^0(D) &= \frac{\mathcal{B}(\bar{B}^0 \to D^+\tau^-\bar{\nu}_\tau)}{\mathcal{B}(\bar{B}^0 \to D^+\ell^-\bar{\nu}_\ell)} = 0.469 \pm 0.084 \pm 0.053,\\
\mathcal{R}^0(D^*) &= \frac{\mathcal{B}(\bar{B}^0 \to D^{*+}\tau^-\bar{\nu}_\tau)}{\mathcal{B}(\bar{B}^0 \to D^{*+}\ell^-\bar{\nu}_\ell)} = 0.355 \pm 0.039 \pm 0.021.
\end{aligned} \tag{1}$$

(The first and second errors are the statistic and systematic uncertainties, respectively.) The measurements have been estimated to deviate at the global level of 3.4σ with respect to SM predictions [1,2]. Therefore, there is the possibility that semileptonic processes involving heavy quarks and the τ lepton are unveiling the effects of particles with large couplings to the heavier fermions, as it is natural for charged scalars which could contribute to the tree-level $b \to c\ell\bar{\nu}$ transitions [2–9].

Before the observation of these possible hints of new physics (NP) in semileptonic $b \to c$ decays, the first experimental analyses of the purely leptonic $B^- \to \tau^-\bar{\nu}_\tau$ mode also reported an excess of events. In the SM, the $\mathcal{B}(B^- \to \tau^-\bar{\nu}_\tau)$ branching fraction is given by

$$\mathcal{B}(B^- \to \tau^-\bar{\nu}_\tau) = \frac{G_F^2 m_B m_\tau^2}{8\pi}\left(1 - \frac{m_\tau^2}{m_B^2}\right)^2 f_B^2 |V_{ub}|^2 \tau_{B^-}, \tag{2}$$

neglecting a tiny electromagnetic radiative correction. Using the lattice QCD average for the B-decay constant $f_B = (190.6 \pm 4.7)$ MeV quoted in Ref. [10], and varying the Cabibbo-Kobayashi-Maskawa (CKM) matrix element $|V_{ub}|$ in the range determined from inclusive and exclusive B decays, $|V_{ub}| = 0.0035 \pm 0.0005$, the prediction follows: $\mathcal{B}(B^- \to \tau^-\bar{\nu}_\tau) = (0.79 \pm 0.23) \times 10^{-4}$, in agreement with the outcome of CKM matrix fits [11,12]. This value is smaller by about a factor of 2 than the experimental results reported in Refs. [13–16] and compiled in Ref. [17]: $\mathcal{B}(B^- \to \tau^-\bar{\nu}_\tau) = (1.68 \pm 0.31) \times 10^{-4}$. However, new Belle [18] and *BABAR* [19] measurements obtained using the hadronic tagging method,

$$\begin{aligned}
\mathcal{B}(B^- \to \tau^-\bar{\nu}_\tau) &= (0.72^{+0.27}_{-0.25} \pm 0.11) \times 10^{-4} \quad \text{(Belle)}\\
\mathcal{B}(B^- \to \tau^-\bar{\nu}_\tau) &= (1.83^{+0.53}_{-0.49} \pm 0.24) \times 10^{-4} \quad (\textit{BABAR}),
\end{aligned} \tag{3}$$

are more consistent with SM, and draw the average $\mathcal{B}(B^- \to \tau^-\bar{\nu}_\tau)$ to a smaller value: $\mathcal{B}(B^- \to \tau^-\bar{\nu}_\tau) = (1.12 \pm 0.22) \times 10^{-4}$, after combination with the semileptonic tagging method results (see Fig. 1).

The different trend of the measurements involving τ in B leptonic and semileptonic decay modes poses two questions. The first one concerns the level of accuracy of the SM predictions for the ratios in Eq. (1). The second one is which kind of new physics effects, if any, could modify the ratios in Eq. (1) without affecting the purely leptonic mode. Indeed, several analyses devoted to trying to explain the anomalies in $B \to D^{(*)}\tau\bar{\nu}_\tau$ within new physics scenarios have considered as possible candidate models, with new scalars having couplings to leptons proportional to the lepton mass, to guarantee the enhancement of the τ modes. This is the case of models with two Higgs doublets, the best-known example being the minimal supersymmetric standard model, in which two Higgs doublets are required to give mass to down-type quarks and charged leptons in one case, and to up-type quarks in the other. In this framework, the ratios of Eq. (1) depend on the mass of the

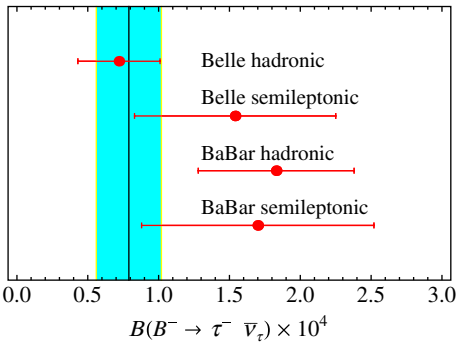

FIG. 1 (color online). Experimental results for $\mathcal{B}(B^- \to \tau^- \bar{\nu}_\tau)$ [14,16,18,19], together with the SM expectation corresponding to $|V_{ub}| = 0.0035 \pm 0.0005$ (vertical band).

charged Higgs $H^\pm$ and the ratio β of the two Higgs doublet vacuum expectation values, and no choice of such parameters allows us to simultaneously reproduce the experimental data on $\mathcal{R}(D)$ and $\mathcal{R}(D^*)$ [1]. Variants of the two Higgs doublet model [4,7], together with other models providing explicit flavor violation [3], might explain the measurements in Eq. (1); however, an enhancement of the purely leptonic B decay rate is generally implied.

In this paper, we reconsider both of the above mentioned issues. We reanalyze the SM prediction for $B \to D^{(*)}\ell\bar{\nu}_\ell$, specifying the main sources of uncertainties and possible improvements. Our results confirm that the most significant deviation is for $\mathcal{R}(D^*)$. Then, we scrutinize the effects of possible NP contributions in the effective weak Hamiltonian having a structure that is able to affect the ratios in Eq. (1) while leaving the pure B leptonic modes unchanged. In particular, we focus on a NP operator constructed from tensor quark and lepton currents. Such operators have been also investigated in Refs. [6,9], but we devote our main attention to differential distributions, namely the lepton forward-backward differential asymmetries, in which the sensitivity to the new Dirac structure is maximal, as emphasized in Ref. [5] for different operators. Although there are scenarios in which tensor operators are generated, in our analysis we do not rely on explicit models: our purpose is to identify physical observables having a mild sensitivity to hadronic uncertainties, which therefore can be used to unveil effects that are easier to interpret. It is only worth mentioning that these operators emerge, for example, in models with new colored bosons carrying both lepton and baryon quantum numbers (referred to as leptoquarks, LQ): $SU(5)_{\rm GUT}$ [20], Pati-Salam $SU(4)$ [21], composite [22], superstrings [23] and technicolor models [24]. In the most general formulation of these models, scalar operators may also occur. Leptoquarks couple to quarks and leptons and, due to limits on flavor-changing neutral currents, preferably to those within the same SM generation. Searches for leptoquarks decaying to 2τ and $2b$ jets, performed by the CMS Collaboration at the CERN LHC, bound (preliminarily) the mass of a possible scalar leptoquark to $M(LQ) > 525$ GeV, and a vector leptoquark to $M(LQ) > 760$ GeV [25]; other bounds can be found in Ref. [26].

In our analysis of semileptonic B decays, we first consider D and D^* mesons in the final state, and then turn to the interesting case of final states with excited positive-parity charmed mesons.

II. EXCLUSIVE $b \to c\ell\bar{\nu}_\ell$ DECAYS

We consider the $b \to c\ell\bar{\nu}_\ell$ effective Hamiltonian comprising the SM term and an additional operator [6,9]:

$$\begin{aligned} H_{\rm eff} &= H_{\rm eff}^{\rm SM} + H_{\rm eff}^{\rm NP} \\ &= \frac{G_F}{\sqrt{2}} V_{cb}[\bar{c}\gamma_\mu(1-\gamma_5)b\bar{\ell}\gamma^\mu(1-\gamma_5)\bar{\nu}_\ell \\ &\quad + \epsilon_T^\ell \bar{c}\sigma_{\mu\nu}(1-\gamma_5)b\bar{\ell}\sigma^{\mu\nu}(1-\gamma_5)\bar{\nu}_\ell]. \end{aligned} \tag{4}$$

G_F is the Fermi constant, and V_{cb} is the CKM matrix element. ϵ_T^ℓ is the relative complex coupling of the new tensor term with respect to the SM one. It is assumed that the main coupling is to the heaviest lepton; hence we set $\epsilon_T^\ell = 0$ for $\ell = e$, μ and $\epsilon_T \equiv \epsilon_T^\tau$. This coupling can be bound experimentally, so that the effects of the new operator can be scrutinized in physical observables which, in general, are expressed as a SM, a new physics, and an interference contribution. For example, the differential $B(p) \to M_c(p')\ell(p_1)\bar{\nu}_\ell(p_2)$ decay rate, with M_c a charmed meson, reads

$$\begin{aligned} &\frac{d\Gamma}{dq^2}(B \to M_c\ell\bar{\nu}_\ell) \\ &= C(q^2)\Big[\frac{d\tilde{\Gamma}}{dq^2}(B \to M_c\ell\bar{\nu}_\ell)|_{\rm SM} + \frac{d\tilde{\Gamma}}{dq^2}(B \to M_c\ell\bar{\nu}_\ell)|_{\rm NP} \\ &\quad + \frac{d\tilde{\Gamma}}{dq^2}(B \to M_c\ell\bar{\nu}_\ell)|_{\rm INT}\Big], \end{aligned} \tag{5}$$

with $q = p - p'$ and $C(q^2)$ defined as

$$C(q^2) = \frac{G_F^2|V_{cb}|^2\lambda^{1/2}(m_B^2, m_{M_c}^2, q^2)}{192\pi^3 m_B^3}\left(1 - \frac{m_\ell^2}{q^2}\right)^2, \tag{6}$$

where $\lambda(x,y,z) = x^2 + y^2 + z^2 - 2(xy + xz + yz)$ is the triangular function. To compute the three terms in Eq. (5), we need the relevant hadronic matrix elements.

A. $B \to D\ell\bar{\nu}_\ell$

The hadronic matrix elements in $B \to D\ell\bar{\nu}_\ell$ can be parametrized in a standard way:

$$\begin{aligned} \langle D(p')|\bar{c}\gamma_\mu b|B(p)\rangle &= F_1(q^2)(p+p')_\mu \\ &\quad + \frac{m_B^2 - m_D^2}{q^2}[F_0(q^2) - F_1(q^2)]q_\mu, \end{aligned} \tag{7}$$

$$\langle D(p')|\bar{c}\sigma_{\mu\nu}(1-\gamma_5)b|B(p)\rangle = \frac{F_T(q^2)}{m_B+m_D}\epsilon_{\mu\nu\alpha\beta}p'^{\alpha}p^{\beta} + i\frac{G_T(q^2)}{m_B+m_D}(p_\mu p'_\nu - p_\nu p'_\mu), \tag{8}$$

(with $F_T = G_T$ from the relation $\sigma_{\mu\nu}\gamma_5 = \frac{i}{2}\epsilon_{\mu\nu\alpha\beta}\sigma^{\alpha\beta}$), so that the three terms in Eq. (5) read

$$\frac{d\tilde{\Gamma}}{dq^2}(B\to D\ell\bar{\nu}_\ell)|_{\rm SM} = \lambda(m_B^2, m_D^2, q^2)\left(1+\frac{m_\ell^2}{2q^2}\right)[F_1(q^2)]^2 + m_B^4\left(1-\frac{m_D^2}{m_B^2}\right)^2\frac{3m_\ell^2}{2q^2}[F_0(q^2)]^2, \tag{9}$$

$$\frac{d\tilde{\Gamma}}{dq^2}(B\to D\ell\bar{\nu}_\ell)|_{\rm NP} = \frac{|\epsilon_T|^2}{2}\frac{q^2}{(m_B+m_D)^2}\lambda(m_B^2, m_D^2, q^2)\left(1+2\frac{m_\ell^2}{q^2}\right)\times[F_T(q^2)+G_T(q^2)]^2, \tag{10}$$

$$\frac{d\tilde{\Gamma}}{dq^2}(B\to D\ell\bar{\nu}_\ell)|_{\rm INT} = -3\,{\rm Re}[\epsilon_T]\frac{m_\ell}{m_B+m_D}\lambda(m_B^2, m_D^2, q^2)\times F_1(q^2)[F_T(q^2)+G_T(q^2)]. \tag{11}$$

In the infinite heavy-quark mass limit, formalized by the heavy-quark effective theory, the form factors in Eqs. (7) and (8) can all be related to the Isgur-Wise function ξ [27]. The result is known [28,29]; expressing $F_1(q^2)$ and $F_0(q^2)$ in terms of two other form factors $h_+(w)$ and $h_-(w)$,

$$F_1(q^2) = \frac{1}{2\sqrt{m_B m_D}}[(m_B+m_D)h_+(w) - (m_B-m_D)h_-(w)], \tag{12}$$

$$\frac{m_B^2-m_D^2}{q^2}[F_0(q^2)-F_1(q^2)] = \frac{1}{2\sqrt{m_B m_D}}[(m_B+m_D)h_-(w) - (m_B-m_D)h_+(w)], \tag{13}$$

and defining the meson momenta in terms of four-velocities, $p = m_B v$ and $p' = m_D v'$, with $w = v\cdot v'$ and $q^2 = m_B^2 + m_D^2 - 2m_B m_D w$, at the leading order in the heavy-quark and α_s expansion, one has

$$h_+(w) = \xi(w), \qquad h_-(w) = 0, \tag{14}$$

with $\xi(w)$ being the Isgur-Wise function. Also, the form factors in Eq. (8) are related to $\xi(w)$ at the same-order expansion:

$$F_T(q^2) = G_T(q^2) = \frac{m_B+m_D}{\sqrt{m_B m_D}}\xi(w). \tag{15}$$

At the next-to-leading order, corrections must be taken into account, which at first are needed for the study of the decay in the SM. We elaborate a determination of the functions h_+, h_- and ξ based on a combination of experimental and theoretical information. The experimental input comes from the *BABAR* analysis of $B\to D\mu\bar{\nu}_\mu$ [30], the differential rate of which, neglecting the lepton mass, reads

$$\frac{d\Gamma}{dw}(B\to D\ell\bar{\nu}_\ell) = \frac{G_F^2|V_{cb}|^2}{48\pi^3}m_B^5 r^3(1+r)^2(w^2-1)^{3/2}\times[F_D(w)]^2, \tag{16}$$

with

$$F_D(w) = \left[h_+(w) - \frac{1-r}{1+r}h_-(w)\right] \tag{17}$$

and $r = \frac{m_D}{m_B}$. Using the parametrization [31]

$$F_D(w) = F_D(1)\{1-8\rho_1^2 z + (51\rho_1^2-10)z^2 - (252\rho_1^2-84)z^3\} \tag{18}$$

in terms of the variable

$$z = \frac{\sqrt{w+1}-\sqrt{2}}{\sqrt{w+1}+\sqrt{2}} \tag{19}$$

from the fit of the product $G^{BABAR}(w) = F_D(w)|V_{cb}|$, the *BABAR* Collaboration provides the parameters $G^{BABAR}(1) = F_D(1)|V_{cb}|$ and ρ_1^2. The outcome of the fit is slightly different for B^- or $\bar{B}^0$ modes; we consider for definiteness the $\bar{B}^0$ case [30],[1]

$$G^{BABAR}(1) = (44.9 \pm 3.2 \pm 1.6)10^{-3}, \qquad \rho_1^2 = 1.29 \pm 0.14 \pm 0.05. \tag{20}$$

This result can be translated into a determination of $\xi(w)$, expressing the form factors $h_\pm(w)$ in terms of the Isgur-Wise function and including the α_s and $1/m_{b,c}$ corrections worked out by M. Neubert in Ref. [28] and by I. Caprini *et al.* in Ref. [31]:

$$h_+(w) = \left[C_1 + \frac{w+1}{2}(C_2+C_3) + (\epsilon_b+\epsilon_c)L_1\right]\xi(w) = \tilde{h}_+(w)\xi(w), \tag{21}$$

$$h_-(w) = \left[\frac{w+1}{2}(C_2-C_3) + (\epsilon_c-\epsilon_b)L_4\right]\xi(w) = \tilde{h}_-(w)\xi(w), \tag{22}$$

[1]The average between the charged and neutral B decay modes is quoted as $G^{BABAR}(1) = (42.3 \pm 1.9 \pm 1.4)10^{-3}$, $\rho_1^2 = 1.20 \pm 0.09 \pm 0.04$.

with $\epsilon_b = \frac{1}{2m_b}$, $\epsilon_c = \frac{1}{2m_c}$. The coefficients $C_{1,2,3}$ and L_i are collected in Appendix A. The C_i terms account for the perturbative corrections, and the L_i terms for the heavy-quark mass corrections; they depend on the hadronic parameter $\bar{\Lambda}$, the difference between the heavy-meson (B, D) and heavy-quark (b, c) masses in the heavy-quark limit. We use $m_b = 4.8$ GeV and $m_c = 1.4$ GeV, and a conservative value $\bar{\Lambda} = 0.5 \pm 0.2$ GeV [28], so that the uncertainty in $\bar{\Lambda}$ encompasses the error on $\bar{\Lambda}/m_b$ and $\bar{\Lambda}/m_c$. The Isgur-Wise function $\xi(w)$ resulting from

$$|V_{cb}|\xi(w) = \frac{G^{BABAR}(w)}{[\tilde{h}_+(w) - \frac{1-r}{1+r}\tilde{h}_-(w)]} \tag{23}$$

is depicted in Fig. 2 (left panel).

The form factors needed for analysis of the mode with τ can be separately derived, using Eqs. (21) and (22) again:

$$|V_{cb}|h_+(w) = \frac{1}{1 - \frac{1-r}{1+r}A(w)} G^{BABAR}(w), \tag{24}$$

$$|V_{cb}|h_-(w) = \frac{A(w)}{1 - \frac{1-r}{1+r}A(w)} G^{BABAR}(w), \tag{25}$$

with $A = \tilde{h}_-/\tilde{h}_+$. For the matrix elements of the tensor operator, we use $\xi(w)$ also in Eq. (15). In the standard model, the results for the semileptonic $\bar{B}^0 \to D^+$ branching fractions can be quoted as

$$\mathcal{B}(\bar{B}^0 \to D^+ \ell^- \bar{\nu}_\ell)|_{\rm SM} = (2.15 \pm 0.45) \times 10^{-2}, \tag{26}$$

$$\mathcal{B}(\bar{B}^0 \to D^+ \tau^- \bar{\nu}_\tau)|_{\rm SM} = (0.70 \pm 0.12) \times 10^{-2}, \tag{27}$$

and, taking the correlation between the predictions for ℓ and τ into account,

$$\mathcal{R}^0(D)|_{\rm SM} = \frac{\mathcal{B}(\bar{B}^0 \to D^+ \tau^- \bar{\nu}_\tau)}{\mathcal{B}(\bar{B}^0 \to D^+ \ell^- \bar{\nu}_\ell)}\Bigg|_{\rm SM} = 0.324 \pm 0.022. \tag{28}$$

The SM prediction for $\mathcal{R}^0(D)$ deviates from the measurement in Eq. (1) (with statistic and systematic uncertainties combined in quadrature) by about 1.5σ. The deviation is smaller in the charged $\mathcal{R}^-(D)$ case.

The stability of Eq. (28) against changes of the input information on form factors is noticeable: sensitivity to $1/m_Q$ corrections can be estimated by varying $\bar{\Lambda}$, and this modifies the central value at the level of a few per mil. Sensitivity to the radiative corrections can be assessed by changing the scale in α_s as indicated in Appendix A, and these corrections are not effective either. Since the value at zero recoil, $G^{BABAR}(1)$, cancels out in the ratio, the main uncertainty in Eq. (28) comes from the error on the parameter ρ_1^2 experimentally determined. The value of $\mathcal{R}^0(D)$ coincides with the one obtained using the form factors F_1 and F_0 from lattice QCD with finite quark masses [6].

B. $B \to D^* \ell \bar{\nu}_\ell$

While the results for $\mathcal{R}^0(D)$ and $\mathcal{R}^-(D)$ do not display a statistically significant deviation from the SM expectation, the case of $\mathcal{R}^0(D^*)$, $\mathcal{R}^-(D^*)$ is quite different. The standard parameterization of the $B \to D^*$ matrix element in terms of form factors is

$$\begin{aligned}\langle D^*(p', \epsilon)|\bar{c}\gamma_\mu(1-\gamma_5)b|\bar{B}(p)\rangle &= -\frac{2V(q^2)}{m_B + m_{D^*}} i\epsilon_{\mu\nu\alpha\beta}\epsilon^{*\nu}p^\alpha p'^\beta \\ &- \Big\{(m_B + m_{D^*})\Big[\epsilon^*_\mu - \frac{(\epsilon^* \cdot q)}{q^2}q_\mu\Big]A_1(q^2) \\ &- \frac{(\epsilon^* \cdot q)}{m_B + m_{D^*}}\Big[(p+p')_\mu - \frac{m_B^2 - m_{D^*}^2}{q^2}q_\mu\Big]A_2(q^2) \\ &+ (\epsilon^* \cdot q)\frac{2m_{D^*}}{q^2}q_\mu A_0(q^2)\Big\}\end{aligned} \tag{29}$$

[with the condition $A_0(0) = \frac{m_B + m_{D^*}}{2m_{D^*}}A_1(0) - \frac{m_B - m_{D^*}}{2m_{D^*}}A_2(0)$], and

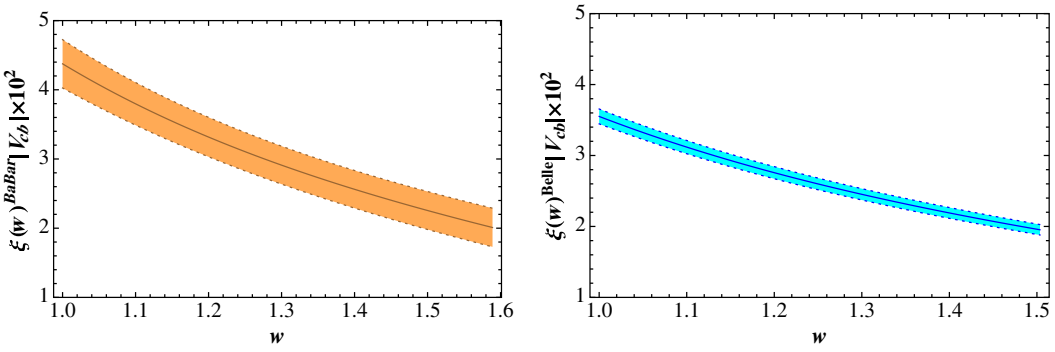

FIG. 2 (color online). The Isgur-Wise function $\xi(w)$ (times $|V_{cb}| \times 10^2$) obtained using the *BABAR* data on $\bar{B}^0 \to D^+ \ell^- \bar{\nu}_\ell$ (left) and the Belle data on $\bar{B}^0 \to D^{*+} \ell^- \bar{\nu}_\ell$ (right). The width of the curves is due to the errors in the parameters fitted in the two cases and to the uncertainty on $\bar{\Lambda}$ and α_s in the determination of the form factor.

$$\langle D^*(p',\epsilon)|\bar{c}\sigma_{\mu\nu}(1-\gamma_5)b|\bar{B}(p)\rangle$$
$$= T_0(q^2)\frac{\epsilon^*\cdot q}{(m_B+m_{D^*})^2}\epsilon_{\mu\nu\alpha\beta}p^\alpha p'^\beta + T_1(q^2)\epsilon_{\mu\nu\alpha\beta}p^\alpha\epsilon^{*\beta} + T_2(q^2)\epsilon_{\mu\nu\alpha\beta}p'^\alpha\epsilon^{*\beta} + i\Big[T_3(q^2)(\epsilon^*_\mu p_\nu - \epsilon^*_\nu p_\mu) + T_4(q^2)(\epsilon^*_\mu p'_\nu - \epsilon^*_\nu p'_\mu) + T_5(q^2)\frac{\epsilon^*\cdot q}{(m_B+m_{D^*})^2}(p_\mu p'_\nu - p_\nu p'_\mu)\Big] \quad (30)$$

with ϵ the D^* polarization vector. We choose the helicity basis for D^*:

$$\epsilon^\mu_L = \frac{1}{m_{D^*}}(|\vec{p}'|,0,0,E'), \qquad \epsilon^\mu_\pm = \frac{1}{\sqrt{2}}(0,1,\mp i,0), \quad (31)$$

where E' and $\vec{p}'$ are the D^* energy and 3-momentum in the B rest frame [$E'=\sqrt{m^2_{D^*}+|\vec{p}'|^2}$, and $|\vec{p}'| = \lambda(m_B^2,m_{D^*}^2,q^2)/2m_B$]. The conditions $\epsilon^\mu_a\cdot p'=0$ and $\epsilon^\mu_a\cdot\epsilon_{\mu,b}=-\delta_{ab}$ with $a,b=L,\pm$ are fulfilled. The differential decay rates for the longitudinal and the transverse D^* polarization in terms of form factors are obtained from

$$\frac{d\tilde{\Gamma}_L}{dq^2}(B\to D^*\ell\bar{\nu}_\ell)|_{\rm SM} = \frac{1}{4m^2_{D^*}}\Big\{6\lambda(m_B^2,m_{D^*}^2,q^2)m^2_{D^*}\frac{m^2_\ell}{q^2}[A_0(q^2)]^2 + \Big(1+\frac{m^2_\ell}{2q^2}\Big)\Big[(m_B+m_{D^*})(m_B^2-m_{D^*}^2-q^2)A_1(q^2) - \frac{\lambda(m_B^2,m_{D^*}^2,q^2)}{m_B+m_{D^*}}A_2(q^2)\Big]^2\Big\}, \quad (32)$$

$$\frac{d\tilde{\Gamma}_L}{dq^2}(B\to D^*\ell\bar{\nu}_\ell)|_{\rm NP} = |\epsilon_T|^2\frac{q^2}{8}\Big(1+\frac{2m^2_\ell}{q^2}\Big)\Big[\frac{\lambda(m_B^2,m_{D^*}^2,q^2)}{m_{D^*}(m_B+m_{D^*})^2}\tilde{T}_0(q^2) + 2\frac{m_B^2+m_{D^*}^2-q^2}{m_{D^*}}\tilde{T}_1(q^2) + 4m_{D^*}\tilde{T}_2(q^2)\Big]^2, \quad (33)$$

$$\frac{d\tilde{\Gamma}_L}{dq^2}(B\to D^*\ell\bar{\nu}_\ell)|_{\rm INT} = -{\rm Re}(\epsilon_T)\frac{3m_\ell}{4(m_B+m_{D^*})}[(m_B+m_{D^*})^2(m_B^2-m_{D^*}^2-q^2)\times A_1(q^2) - \lambda(m_B^2,m_{D^*}^2,q^2)A_2(q^2)] \times\Big[\frac{\lambda(m_B^2,m_{D^*}^2,q^2)}{m^2_{D^*}(m_B+m_{D^*})^2}\tilde{T}_0(q^2) + \frac{2(m_B^2+m_{D^*}^2-q^2)}{m^2_{D^*}} \times\tilde{T}_1(q^2) + 4\tilde{T}_2(q^2)\Big], \quad (34)$$

$$\frac{d\tilde{\Gamma}_\pm}{dq^2}(B\to D^*\ell\bar{\nu}_\ell)|_{\rm SM} = q^2\Big(1+\frac{m^2_\ell}{2q^2}\Big)\Big\{(m_B+m_{D^*})^2[A_1(q^2)]^2 + \frac{\lambda(m_B^2,m_{D^*}^2,q^2)}{(m_B+m_{D^*})^2}[V(q^2)]^2\Big\}, \quad (35)$$

$$\frac{d\tilde{\Gamma}_\pm}{dq^2}(B\to D^*\ell\bar{\nu}_\ell)|_{\rm NP} = |\epsilon_T|^2\Big(1+\frac{2m^2_\ell}{q^2}\Big)\{\lambda(m_B^2,m_{D^*}^2,q^2)[\tilde{T}_1(q^2)+\tilde{T}_2(q^2)]^2 + 2q^2[m_B^2[\tilde{T}_1(q^2)]^2 + m^2_{D^*}[\tilde{T}_2(q^2)]^2 + (m_B^2+m_{D^*}^2-q^2)\tilde{T}_1(q^2)\tilde{T}_2(q^2)]\}, \quad (36)$$

$$\frac{d\tilde{\Gamma}_\pm}{dq^2}(B\to D^*\ell\bar{\nu}_\ell)|_{\rm INT} = -{\rm Re}(\epsilon_T)3m_\ell\Big\{2q^2(m_B+m_{D^*})A_1(q^2)\tilde{T}_1(q^2) + \Big[(m_B+m_{D^*})(m_B^2-m_{D^*}^2-q^2)A_1(q^2) - \frac{\lambda(m_B^2,m_{D^*}^2,q^2)}{(m_B+m_{D^*})}V(q^2)\Big][\tilde{T}_1(q^2)+\tilde{T}_2(q^2)]\Big\}, \quad (37)$$

to be multiplied by the factor $C(q^2)$ in Eq. (6). We have used the combinations

$$\tilde{T}_0(q^2) = T_0(q^2) - T_5(q^2), \quad \tilde{T}_1(q^2) = T_1(q^2) + T_3(q^2), \quad \tilde{T}_2(q^2) = T_2(q^2) + T_4(q^2). \quad (38)$$

At the leading order in the heavy-quark expansion, the form factors in Eqs. (29) and (30) are related to the Isgur-Wise function, while other contributions appear at the next-to-leading order. Analogously to the decay to D, one expresses V and A_i in terms of the form factors h_V and h_{A_i}:

$$V(q^2) = \frac{m_B+m_{D^*}}{2\sqrt{m_Bm_{D^*}}}h_V(w),$$
$$A_1(q^2) = \sqrt{m_Bm_{D^*}}\frac{w+1}{m_B+m_{D^*}}h_{A_1}(w),$$
$$A_2(q^2) = \frac{m_B+m_{D^*}}{2\sqrt{m_Bm_{D^*}}}\Big[h_{A_3}(w)+\frac{m_{D^*}}{m_B}h_{A_2}(w)\Big], \quad (39)$$
$$A_0(q^2) = \frac{1}{2\sqrt{m_Bm_{D^*}}}[m_B(w+1)h_{A_1}(w) - (m_B-m_{D^*}w)h_{A_2}(w) - (m_Bw-m_{D^*})h_{A_3}(w)],$$

with $q^2 = m_B^2+m^2_{D^*}-2m_Bm_{D^*}w$. Including α_s and $\frac{1}{m_b}$ and $\frac{1}{m_c}$ corrections, the relations have been worked out [28,31]:

$$h_V(w) = [C_1+\epsilon_c(L_2-L_5)+\epsilon_b(L_1-L_4)]\xi(w), \quad (40)$$

$$h_{A_1}(w) = \left[C_1^5 + \epsilon_c\left(L_2 - \frac{w-1}{w+1}L_5\right) + \epsilon_b\left(L_1 - \frac{w-1}{w+1}L_4\right)\right]\xi(w), \tag{41}$$

$$h_{A_2}(w) = [C_2^5 + \epsilon_c(L_3 + L_6)]\xi(w), \tag{42}$$

$$h_{A_3}(w) = [C_1^5 + C_3^5 + \epsilon_c(L_2 - L_3 - L_5 + L_6) + \epsilon_b(L_1 - L_4)]\xi(w). \tag{43}$$

The expressions of C_i, which incorporate the radiative corrections, and L_i are collected in Appendix A: the L_i terms account for the $\mathcal{O}(1/m_Q)$ corrections in the heavy-quark expansion, and are determined from QCD sum rule analyses of the subleading form factors [28]. On the other hand, the relations of the form factors T_i in Eq. (30) to $\xi(w)$ in the heavy-quark limit are

$$T_0(q^2) = T_5(q^2) = 0, \qquad T_1(q^2) = T_3(q^2) = \sqrt{\frac{m_{D^*}}{m_B}}\xi(w),$$
$$T_2(q^2) = T_4(q^2) = \sqrt{\frac{m_B}{m_{D^*}}}\xi(w); \tag{44}$$

we use these expressions in the analysis of the tensor operator.

Let us focus on the SM. Due to the heavy-quark spin symmetry, a unique form factor describes both $B \to D$ and $B \to D^*$ transitions, so that we could use the Isgur-Wise function found in the previous section. To partially take into account the different experimental systematics, we choose to use the determination of ξ obtained by the Belle Collaboration from the analysis of $\bar{B}^0 \to D^{*+}\mu\bar{\nu}_\mu$ [32], for which the differential decay rate, neglecting the lepton mass, is

$$\frac{d\Gamma}{dw}(B \to D^*\ell\bar{\nu}_\ell) = \frac{G_F^2|V_{cb}|^2}{48\pi^3}(m_B - m_{D^*})^2 m_{D^*}^3 \mathcal{G}(w)\mathcal{F}^2(w), \tag{45}$$

with

$$\mathcal{G}(w)\mathcal{F}^2(w) = h_{A_1}^2(w)\sqrt{w^2-1}(w+1)^2\left\{2\left[\frac{1-2wr^*+r^{*2}}{(1-r^*)^2}\right]\times\left[1 + R_1(w)^2\frac{w-1}{w+1}\right] + \left[1 + (1-R_2(w))\frac{w-1}{1-r^*}\right]^2\right\}. \tag{46}$$

In Eq. (46), $r^* = \frac{m_{D^*}}{m_B}$, and $\mathcal{G}$, R_1 and R_2 are given by

$$\mathcal{G}(w) = \sqrt{w^2-1}(w+1)^2\left[1 + 4\frac{w}{w+1}\frac{1-2wr^*+r^{*2}}{(1-r^*)^2}\right],$$
$$R_1(w) = (R^*)^2\frac{w+1}{2}\frac{V(w)}{A_1(w)}, \tag{47}$$
$$R_2(w) = (R^*)^2\frac{w+1}{2}\frac{A_2(w)}{A_1(w)},$$

with $R^* = 2\frac{\sqrt{m_B m_{D^*}}}{m_B + m_{D^*}}$. The three unknown functions in Eqs. (46) and (47) have been determined by Belle adopting the parametrization [31]

$$h_{A_1}(w) = h_{A_1}(1)[1 - 8\rho^2 z + (53\rho^2 - 15)z^2 - (231\rho^2 - 91)z^3], \tag{48}$$

$$R_1(w) = R_1(1) - 0.12(w-1) + 0.05(w-1)^2, \tag{49}$$

$$R_2(w) = R_1(1) + 0.11(w-1) - 0.06(w-1)^2, \tag{50}$$

[with z defined in Eq. (19)]. The fit of the parameters in Eqs. (48)–(50) is quoted as [32]

$$\begin{aligned}\mathcal{F}(1)|V_{cb}| &= (34.6 \pm 0.2 \pm 1.0) \times 10^{-3},\\ \rho^2 &= 1.214 \pm 0.034 \pm 0.009,\\ R_1(1) &= 1.401 \pm 0.034 \pm 0.018,\\ R_2(1) &= 0.864 \pm 0.024 \pm 0.008.\end{aligned} \tag{51}$$

From these expressions one can reconstruct $\xi(w)$,

$$h_{A_1}(w) = \tilde{h}_{A_1}(w)\xi(w), \tag{52}$$

with $\tilde{h}_{A_1}$ defined through Eq. (41). The fit provides us with the determination depicted in Fig. 2 (right panel). Through Eqs. (40), (42), and (43), the form factors h_V, h_{A_2} and h_{A_3} can be reconstructed, including the NLO $1/m_Q$ and α_s corrections, and $\mathcal{B}(\bar{B}^0 \to D^{*+}\tau^-\bar{\nu}_\ell)$ can be computed. The results are

$$\begin{aligned}\mathcal{B}(\bar{B}^0 \to D^{*+}\ell^-\bar{\nu}_\ell)|_{\rm SM} &= (4.62 \pm 0.33) \times 10^{-2},\\ \mathcal{B}(\bar{B}^0 \to D^{*+}\tau^-\bar{\nu}_\tau)|_{\rm SM} &= (1.16 \pm 0.08) \times 10^{-2},\end{aligned} \tag{53}$$

and, taking the correlation between the predictions for the ℓ and τ modes into account,

$$\mathcal{R}^0(D^*)|_{\rm SM} = \left.\frac{\mathcal{B}(\bar{B}^0 \to D^{*+}\tau^-\bar{\nu}_\tau)}{\mathcal{B}(\bar{B}^0 \to D^{*+}\ell^-\bar{\nu}_\ell)}\right|_{\rm SM} = 0.250 \pm 0.003. \tag{54}$$

The result in Eq. (54) deviates from the measurement in Eq. (1) (with statistic and systematic errors combined in quadrature) by 2.3σ. It coincides with the measurement in Refs. [2,7,9], due to the stability of the ratio $\mathcal{R}^0(D^*)$ against changes of the input parameters: varying the central value of $\bar{\Lambda}$ and of the quark masses by 30% produces less than 1% variation in the result. The radiative corrections, changing the scale in α_s as mentioned in

Appendix A, do not produce an appreciable variation of the result. On the other hand, in the individual branching fractions there is a mild sensitivity to $\bar{\Lambda}$: by setting this parameter to zero (i.e., ignoring $1/m_Q$ corrections), the branching fractions in Eq. (53) are reduced by about 5%. In the charged case, there is a deviation of 1.8σ between the SM prediction for $\mathcal{R}(D^*)$ and the measurement in Eq. (1).

III. EFFECTS OF THE TENSOR OPERATOR ON $\mathcal{R}(D^{(*)})$ AND OTHER OBSERVABLES

If the tensions in $\mathcal{R}(D)$ and $\mathcal{R}(D^*)$ are due to NP effects, it is interesting to investigate the new operator in the effective Hamiltonian [Eq. (4)] which affects the observables in $B \to D^{(*)}\tau\nu_\tau$ transitions, focusing on the signatures with minimal dependence on hadronic quantities. As in Refs. [2–7,9], $\mathcal{R}(D)$ and $\mathcal{R}(D^*)$ data allow us to constrain the values of the new effective dimensionless coupling. In our case, ϵ_T is bounded as shown in Fig. 3. Using the parameterization

$$\epsilon_T = |a_T| e^{i\theta} + \epsilon_{T0}, \tag{55}$$

the tightest bound to ϵ_{T0} and $|a_T|$ is obtained from the measurement of $\mathcal{R}(D^*)$, while the combination of $\mathcal{R}(D)$ and $\mathcal{R}(D^*)$ data fixes the range of the phase θ. We select the overlap of the two regions determined by $\mathcal{R}(D)$ and $\mathcal{R}(D^*)$ both at 1σ. In this overlap region, the function $\chi^2(\epsilon_T) = (\frac{\mathcal{R}(D,\epsilon)-\mathcal{R}(D)^{\rm exp}}{\Delta\mathcal{R}(D)^{\rm exp}})^2 + (\frac{\mathcal{R}(D^*,\epsilon)-\mathcal{R}(D^*)^{\rm exp}}{\Delta\mathcal{R}(D^*)^{\rm exp}})^2$ has values running between 1.51 and 1.75. This permitted range of ϵ_T is represented as

$$\begin{aligned} &\mathrm{Re}[\epsilon_{T0}] = 0.17, \qquad \mathrm{Im}[\epsilon_{T0}] = 0, \\ &|a_T| \in [0.24, 0.27], \qquad \theta \in [2.6, 3.7]\ \mathrm{rad} \end{aligned} \tag{56}$$

and is also depicted in Fig. 3. By varying the effective coupling in this region, we can analyze the impact of the new operator on various differential distributions.

We start with the longitudinal and transverse D^* polarization distributions in $B \to D^*\tau\bar{\nu}_\tau$. We consider the decay to a D^* with definite helicity, with differential decay width $\frac{d\Gamma_{L,\pm}}{dq^2}$ for the three cases L, $\pm$. We define $\frac{d\Gamma_T}{dq^2} = \frac{d\Gamma_+}{dq^2} + \frac{d\Gamma_-}{dq^2}$ and show in Fig. 4 the differential branching fractions. The uncertainty in the distributions reflects the uncertainty on the parameters of the Belle Isgur-Wise function, on $\bar{\Lambda}$, and—in the case of NP—on ϵ_T. While the shapes of the distributions are slightly modified from SM to NP, the maxima increase, a consequence of the increase of the branching fractions.

The differential decay width distributions for D and D^* (summed over the D^* polarizations) have been measured by *BABAR* [33] and can be compared to the SM and NP scenario predictions. Once normalized to the total number of events, not only are the SM distributions compatible with data, as is remarked in Ref. [33], but also the distributions in the considered NP scenario agree with measurements, as one can argue considering Fig. 5. This confirms that the shape of such distributions does not allow us at present to select between these possibilities, and other observables should be analyzed for a more efficient discrimination.

Other observables are the longitudinal and transverse D^* polarization distributions in $B \to D^*\tau\bar{\nu}_\tau$ normalized to $B \to D^*\ell\bar{\nu}_\ell$. They are defined as

$$R^{D^*}_{L,T}(q^2) = \frac{d\Gamma_{L,T}(B \to D^*\tau\bar{\nu}_\tau)/dq^2}{d\Gamma_{L,T}(B \to D^*\ell\bar{\nu}_\ell)/dq^2}. \tag{57}$$

The SM predictions are shown in Fig. 6, together with the modifications induced by the tensor operator.

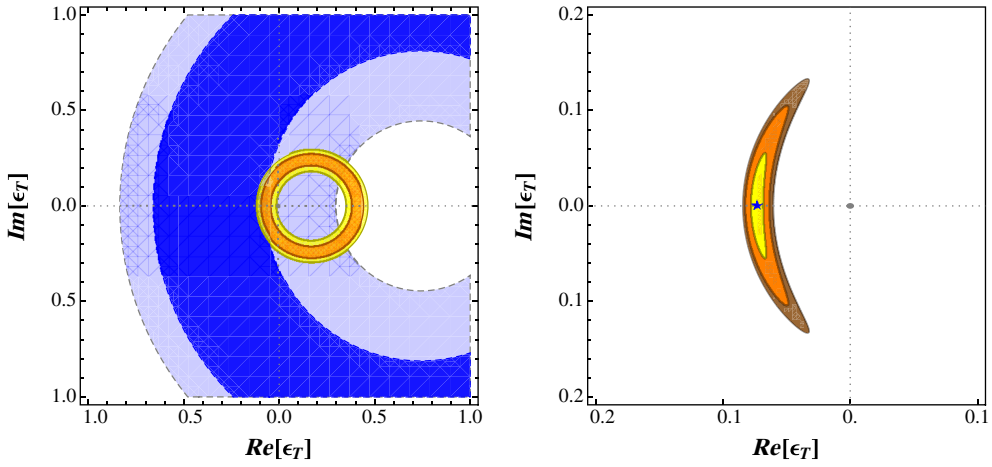

FIG. 3 (color online). *Left:* Regions in the $[\mathrm{Re}(\epsilon_T), \mathrm{Im}(\epsilon_T)]$ plane determined from the experimental data (to 1σ and 2σ) on $\mathcal{R}(D)$ (large rings) and $\mathcal{R}(D^*)$ (small rings). *Right:* Region corresponding to values of χ^2 between the minimum (indicated by the star) and 1.55 (yellow, light), 1.65 (orange, gray), and 1.75 (brown, dark).

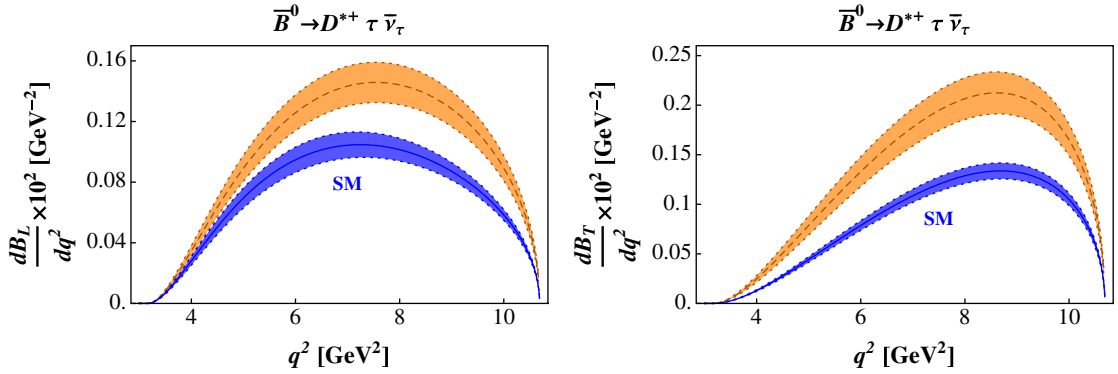

FIG. 4 (color online). Differential branching ratios with polarized D^*: $\frac{d\mathcal{B}(B\to D^*\tau\bar{\nu}_\tau)_L}{dq^2}$ (left) and $\frac{d\mathcal{B}(B\to D^*\tau\bar{\nu}_\tau)_T}{dq^2}$ (right). The lower (blue) bands are the SM prediction; the upper (orange) bands include NP effects. In the SM, the uncertainties on the parameters of the Isgur-Wise function in Eq. (51), together with the errors on $\bar{\Lambda}$ and α_s, are included. In the case of the NP curves, the uncertainty on ϵ_T is also considered.

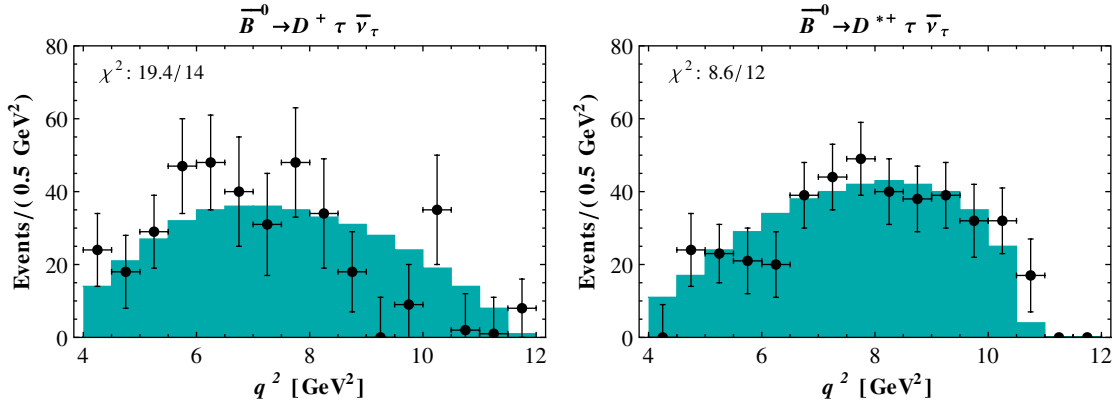

FIG. 5 (color online). $\frac{d\Gamma(B\to D\tau\bar{\nu}_\tau)}{dq^2}$ (left) and $\frac{d\Gamma(B\to D^*\tau\bar{\nu}_\tau)}{dq^2}$ (right) distributions in the NP scenario (for the central value of ϵ_T, shaded histograms) compared to *BABAR* data (points) [33]; the distributions are normalized to the total number of events.

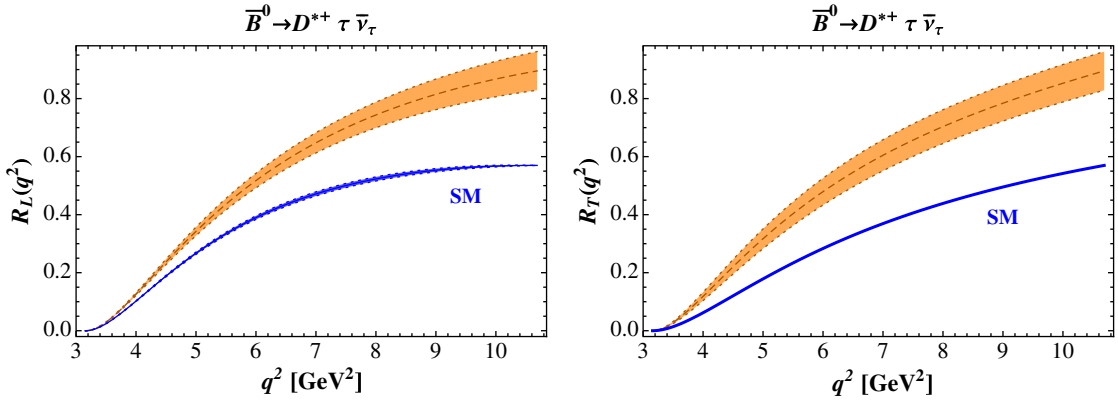

FIG. 6 (color online). D^* polarization ratios $R_L^{D^*}(q^2)$ (left) and $R_T^{D^*}(q^2)$ (right), defined in Eq. (57). Notations are the same as in Fig. 4.

At large q^2, the observables are enhanced by 30%–50%, a noticeable effect. Furthermore, at odds with scenarios in which only R_L is affected by new physics [7], in the case of the tensor operator, both the longitudinal and the transverse R_L and R_T distributions are modified.

The longitudinal and transverse polarization fractions of the D^* meson,

$$F_{L,T}(q^2) = \frac{d\Gamma_{L,T}(B \to D^* \tau \bar{\nu}_\tau)}{dq^2} \times \left(\frac{d\Gamma(B \to D^* \tau \bar{\nu}_\tau)}{dq^2}\right)^{-1}, \tag{58}$$

are shown in Fig. 7. Both the SM and NP predictions are affected by a small error, since in the heavy-quark limit the observables in Eq. (58) are free of hadronic uncertainties, due to the cancellation of the form factor $\xi(w)$ in the ratio. The residual uncertainty reflects that on $\bar{\Lambda}$, which controls the $1/m_Q$ corrections. The uncertainty on $\bar{\Lambda}$ also enters in the curves obtained in the NP scenario in combination with ϵ_T. In the SM, $F_L(q^2)$ ranges between 0.75 at low q^2 and about 0.35 at a high squared-momentum transfer; in NP in the allowed region of ϵ_T, $F_L(q^2)$ is between 0.35 and about 0.65 at low q^2, while this observable converges to the SM value at high q^2. The SM predicts a dominant longitudinal polarization at small q^2; in NP the longitudinal and transverse polarizations have similar fractions up to $q^2 = 6$ GeV^2.

An important observable is the forward-backward $\mathcal{A}_{\rm FB}(q^2)$ asymmetry in $B \to D\tau\bar{\nu}_\tau$ and $B \to D^*\tau\bar{\nu}_\tau$, defined as

$$\mathcal{A}_{\rm FB}(q^2) = \frac{\int_0^1 d\cos\theta_\ell \frac{d\Gamma}{dq^2 d\cos\theta_\ell} - \int_{-1}^0 d\cos\theta_\ell \frac{d\Gamma}{dq^2 d\cos\theta_\ell}}{\frac{d\Gamma}{dq^2}}, \tag{59}$$

where θ_ℓ is the angle between the direction of the charged lepton and the $D^{(*)}$ meson in the lepton-pair rest frame. We use the notation

$$\mathcal{A}_{\rm FB}(q^2) = \frac{1}{\frac{d\Gamma}{dq^2}} \frac{3C(q^2)}{16} \{\tilde{\mathcal{A}}_{\rm FB}^{\rm SM}(q^2) + \tilde{\mathcal{A}}_{\rm FB}^{\rm NP}(q^2) + \tilde{\mathcal{A}}_{\rm FB}^{\rm INT}(q^2)\}, \tag{60}$$

with $C(q^2)$ defined in Eq. (6) and the three terms in the parentheses given for D:

$$\begin{aligned}
\tilde{\mathcal{A}}_{\rm FB}^{\rm SM}(q^2) &= 8F_0(q^2)F_1(q^2)(m_B^2 - m_D^2) \\
&\quad \times \frac{m_\ell^2}{q^2}\left(1 - \frac{m_\ell^2}{q^2}\right)\lambda^{1/2}(m_B^2, m^2, q^2), \\
\tilde{\mathcal{A}}_{\rm FB}^{\rm NP}(q^2) &= 0, \\
\tilde{\mathcal{A}}_{\rm FB}^{\rm INT}(q^2) &= -8\,{\rm Re}(\epsilon_T)F_0(q^2)[F_T(q^2) + G_T(q^2)] \\
&\quad \times (m_B - m_D)m_\ell\left(1 - \frac{m_\ell^2}{q^2}\right)\lambda^{1/2}(m_B^2, m^2, q^2);
\end{aligned} \tag{61}$$

and for D^*:

$$\begin{aligned}
\tilde{\mathcal{A}}_{\rm FB}^{\rm SM}(q^2) &= \frac{4}{m_{D^*}(m_B + m_{D^*})q^2}\left(1 - \frac{m_\ell^2}{q^2}\right)\lambda^{1/2}(m_B^2, m_{D^*}^2, q^2)\{m_\ell^2 A_0(q^2)[A_1(q^2)(m_B + m_{D^*})^2(m_B^2 - m_{D^*}^2 - q^2) \\
&\quad - \lambda(m_B^2, m_{D^*}^2, q^2)A_2(q^2)] - 4m_{D^*}(m_B + m_{D^*})q^4 A_1(q^2)V(q^2)\},
\end{aligned} \tag{62}$$

$$\begin{aligned}
\tilde{\mathcal{A}}_{\rm FB}^{\rm NP}(q^2) &= 16|\epsilon_T|^2 \frac{m_\ell^2}{q^2}\left(1 - \frac{m_\ell^2}{q^2}\right)\lambda^{1/2}(m_B^2, m_{D^*}^2, q^2)(\tilde{T}_1(q^2) + \tilde{T}_2(q^2)) \\
&\quad \times [(m_B^2 - m_{D^*}^2)(\tilde{T}_1(q^2) + \tilde{T}_2(q^2)) + q^2(\tilde{T}_1(q^2) - \tilde{T}_2(q^2))],
\end{aligned} \tag{63}$$

$$\begin{aligned}
\tilde{\mathcal{A}}_{\rm FB}^{\rm INT}(q^2) &= -4\,{\rm Re}(\epsilon_T)m_\ell\left(1 - \frac{m_\ell^2}{q^2}\right)\lambda^{1/2}(m_B^2, m_{D^*}^2, q^2)\Big\{4(m_B + m_{D^*})A_1(q^2)(\tilde{T}_1(q^2) + \tilde{T}_2(q^2)) \\
&\quad + A_0(q^2)\Big[\frac{\lambda(m_B^2, m_{D^*}^2, q^2)}{m_{D^*}(m_B + m_{D^*})^2}\tilde{T}_0(q^2) + 2\frac{m_B^2 + m_{D^*}^2 - q^2}{m_{D^*}}\tilde{T}_1(q^2) + 4m_{D^*}\tilde{T}_2(q^2)\Big] \\
&\quad - \frac{V(q^2)}{m_B + m_{D^*}}[q^2(\tilde{T}_1(q^2) - \tilde{T}_2(q^2)) + (m_B^2 - m_{D^*}^2)(\tilde{T}_1(q^2) + \tilde{T}_2(q^2))]\Big\}.
\end{aligned} \tag{64}$$

In Fig. 8, we plot $\mathcal{A}_{\rm FB}(q^2)$ for $B \to D\tau\bar{\nu}_\tau$ and $B \to D^*\tau\bar{\nu}_\tau$. The SM prediction is affected by almost no theoretical uncertainty, because of a nearly complete cancellation of the hadronic parameters in the ratio. In the case of NP, we have also taken into account the uncertainty on θ and $|a_T|$. The SM curve lies in both cases below the NP distribution for all values of q^2. The most interesting deviation concerns the D^* mode: the SM predicts a zero for $\mathcal{A}_{\rm FB}$ at $q^2 \simeq 6.15$ GeV^2, while in the NP case the zero is shifted towards larger values, $q^2 \in [8.1, 9.3]$ GeV^2. Even though the experimental determination of the zeros of the forward-backward asymmetry is challenging, this observable effectively discriminates the SM from the NP model. The integrated asymmetries, obtained by integrating separately the numerator and the denominator in Eq. (59), are collected in Table I: for D^*, in the NP

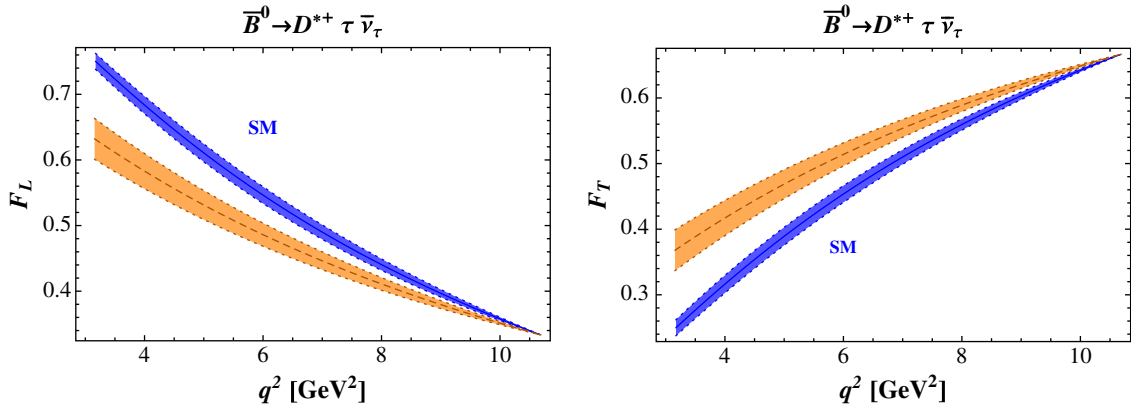

FIG. 7 (color online). Polarization fractions $F_L(q^2)$ (left) and $F_T(q^2)$ (right) for $B \to D^* \tau \bar{\nu}_\tau$, defined in Eq. (58). Notations are the same as in Fig. 4.

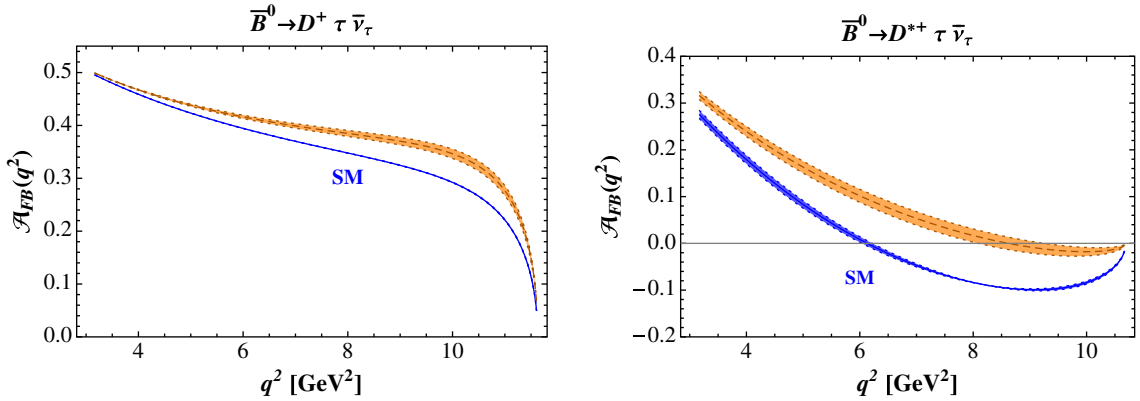

FIG. 8 (color online). Forward-backward asymmetry $\mathcal{A}_{\rm FB}(q^2)$ for $B \to D \tau \bar{\nu}_\tau$ (left) and $B \to D^* \tau \bar{\nu}_\tau$ (right). The lower (blue) curves are the SM predictions; the upper (orange) bands are the NP expectations. Uncertainty on $\bar{\Lambda}$ has been included and, in the case of NP, also uncertainties on the parameters $|a_T|$ and θ.

scenario, the integrated asymmetry has the opposite sign with respect to the SM.

IV. TENSOR OPERATOR IN $B \to D^{**} \ell \bar{\nu}_\ell$ DECAYS

The new operator in the effective Hamiltonian [Eq. (4)] affects other exclusive decay modes that are worth investigating. Of peculiar interest are the semileptonic B and B_s transitions into excited charmed mesons. The lightest multiplet of such hadrons, corresponding to the quark-model p-wave ($\ell = 1$) mesons and generically denoted $D^{**}_{(s)}$, comprises four positive parity states which, in the heavy-quark limit, fill two doublets labeled by the (conserved) angular momentum $\vec{s}_\ell = \vec{s}_q + \vec{\ell}$ ($\vec{s}_q$ is spin of the light antiquark), hence $s_\ell = 1/2$ or $s_\ell = 3/2$. The two mesons belonging to the first doublet, $[D^*_{(s)0}, D'_{(s)1}]$, have spin parity $J^P = (0^+, 1^+)$; the mesons in the second doublet have $J^P = (1^+, 2^+)$ and are named $[D_{(s)1}, D^*_{(s)2}]$. All the members of the doublets, with and without strangeness, have been observed, and the two $s^P_\ell = 1/2^+$ states without strangeness are found to be broad, as expected [34].

In the heavy-quark limit also, the semileptonic B transitions to mesons belonging to the same charmed doublet can be described in terms of a single form factor. B decays to (D^*_0, D'_1) are governed by a universal function denoted as

TABLE I. Integrated forward-backward asymmetry for the considered decay modes. The first row reports the SM results; in the second row, the effect of the tensor operator is included.

	$\bar{B}^0 \to D^+ \tau \bar{\nu}_\tau$	$\bar{B}^0 \to D^{*+} \tau \bar{\nu}_\tau$	$\bar{B}^0 \to D^{*+}_0 \tau \bar{\nu}_\tau$	$\bar{B}^0 \to D'^{+}_1 \tau \bar{\nu}_\tau$	$\bar{B}^0 \to D^{+}_1 \tau \bar{\nu}_\tau$	$\bar{B}^0 \to D^{*+}_2 \tau \bar{\nu}_\tau$
$\mathcal{A}^{\rm SM}_{\rm FB}$	0.357 ± 0.002	-0.040 ± 0.003	0.315	0.026	0.24	0.07
$\mathcal{A}_{\rm FB}$	0.40 ± 0.005	0.048 ± 0.013	0.30 ± 0.005	0.08 ± 0.01	0.21 ± 0.003	0.14 ± 0.01

$\tau_{1/2}(w)$; B decays to (D_1, D_2^*) by the $\tau_{3/2}(w)$ form factor (the matrix elements are collected in Appendix B). There are several determinations of $\tau_i(w)$, parametrized in terms of the zero-recoil value $\tau_i(1)$ [contrary to the Isgur-Wise function, $\tau_i(w)$ are not normalized to unity at $w = 1$], of the slope ρ_i^2 and of the curvature c_i. In the ratios of branching fractions and asymmetries, the zero-recoil value does not play any role, and this reduces the main dependence of the observables on the hadronic parameters. The present experimental situation needs to be settled, since the semileptonic B-decay rates into (D_0^*, D_1') exceed the predictions obtained using computed $\tau_i(1)$; the origin of the discrepancy is still unknown, and could be related to the broad widths of the final charmed mesons, which determine a difficulty in the exclusive reconstruction, or to possible pollution from other (e.g., radial) excited states. Semileptonic B_s decays to $s_\ell^P = 1/2^+$ $c\bar{s}$ mesons could clarify the issue, due to the narrow width of the strange charmed resonances [35]. On the other hand, the tensor operator produces precise correlations among various observables; therefore, its effects could be distinguished from others.

For definiteness, we use a QCD sum rule determination of $\tau_{3/2}(w)$ at leading order in α_s [36,37], and of $\tau_{1/2}(w)$ at $\mathcal{O}(\alpha_s)$ [38]:

$$\tau_{3/2}(w) = \tau_{3/2}(1)[1 - \rho_{3/2}^2(w-1)], \tag{65}$$

$$\tau_{1/2}(w) = \tau_{1/2}(1)[1 - \rho_{1/2}^2(w-1) + c_{1/2}(w-1)^2], \tag{66}$$

with

$$\tau_{3/2}(1) = 0.28, \qquad \rho_{3/2}^2 = 0.9, \tag{67}$$

$$\tau_{1/2}(1) = 0.35 \pm 0.08, \qquad \rho_{1/2}^2 = 2.5 \pm 1.0, \qquad c_{1/2} = 3 \pm 3. \tag{68}$$

The differential decay rates for $B \to D^{**}\ell\bar{\nu}_\ell$ can be written as in Eq. (5); see Appendix B. The ratios

$$\mathcal{R}(D_0^*) = \frac{\mathcal{B}(B \to D_0^*\tau\bar{\nu}_\tau)}{\mathcal{B}(B \to D_0^*\ell\bar{\nu}_\ell)} \tag{69}$$

and the analogous $\mathcal{R}(D_1')$, $\mathcal{R}(D_1)$ and $\mathcal{R}(D_2^*)$ depend on the effective coupling ϵ_T. This also happens in $B_s \to D_s^{**}\ell\bar{\nu}_\ell$ transitions, in the $SU(3)_F$ symmetry limit for the form factors.

In Fig. 9, for each meson doublet we show the correlation between the ratios of Eq. (69) for B and B_s, together with the SM predictions $[\mathcal{R}(D_0^*), \mathcal{R}(D_1')] = (0.077, 0.100)$, $[\mathcal{R}(D_{s0}^*), \mathcal{R}(D_{s1}')] = (0.107, 0.112)$, $[\mathcal{R}(D_1), \mathcal{R}(D_2^*)] = (0.065, 0.059)$ and $[\mathcal{R}(D_{s1}), \mathcal{R}(D_{s2}^*)] = (0.060, 0.055)$. The tensor operator produces a sizeable increase in the ratios $\mathcal{R}$, which is correlated for the two members in each doublet. The hadronic uncertainty is mild: using the τ_i functions in Ref. [39], the results remain almost unchanged in the case of the $s_\ell = 3/2$ doublet, while for $s_\ell = 1/2$ they are smaller by about 25% in the SM and in the NP case. The same effect is found using the form factors obtained by lattice QCD [40].

The differential forward-backward asymmetries in the case of the four positive-parity charmed mesons are collected in Fig. 10, and the integrated ones are given in Table I. While in $B \to (D_0^*, D_1)\tau\bar{\nu}_\tau$ the forward-backward asymmetry does not discriminate between SN and NP, in the modes with D_1' and D_2^* it is a sensitive observable: The inclusion of the tensor operator produces an enhancement of $\mathcal{A}_{\rm FB}$ with respect to SM for all values of q^2. Moreover, in SM there is a zero which, in the case of $B \to D_1'\tau\bar{\nu}_\tau$,

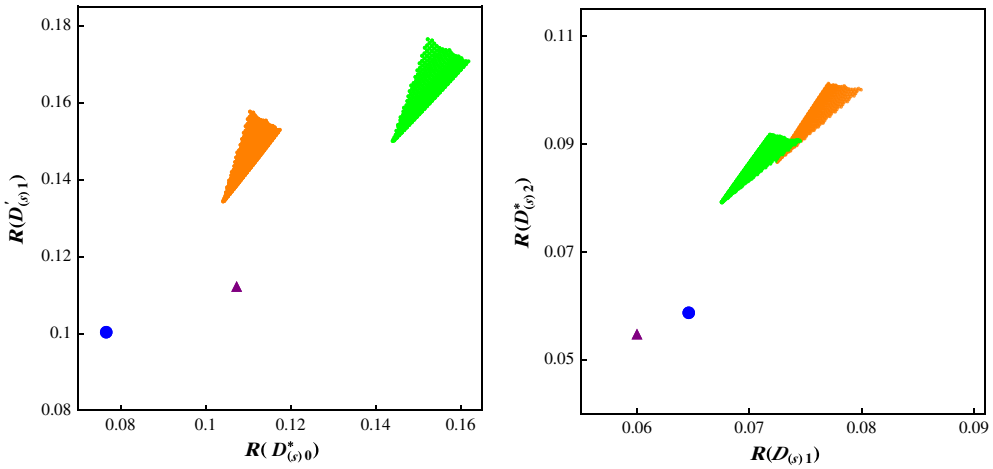

FIG. 9 (color online). *Left:* Correlations between the ratios $\mathcal{R}(D_{(s)0}^*)$ and $\mathcal{R}(D_{(s)1}')$ for mesons belonging to the $[D_{(s)0}^*, D_{(s)1}']$ doublet, without (orange, dark) and with strangeness (green, light). *Right:* Correlations between $\mathcal{R}(D_{(s)1})$ and $\mathcal{R}(D_{(s)2}^*)$ for mesons in the $[D_{(s)1}, D_{(s)2}^*]$ doublet. The dots (triangles) correspond to the SM results for mesons without (with) strangeness.

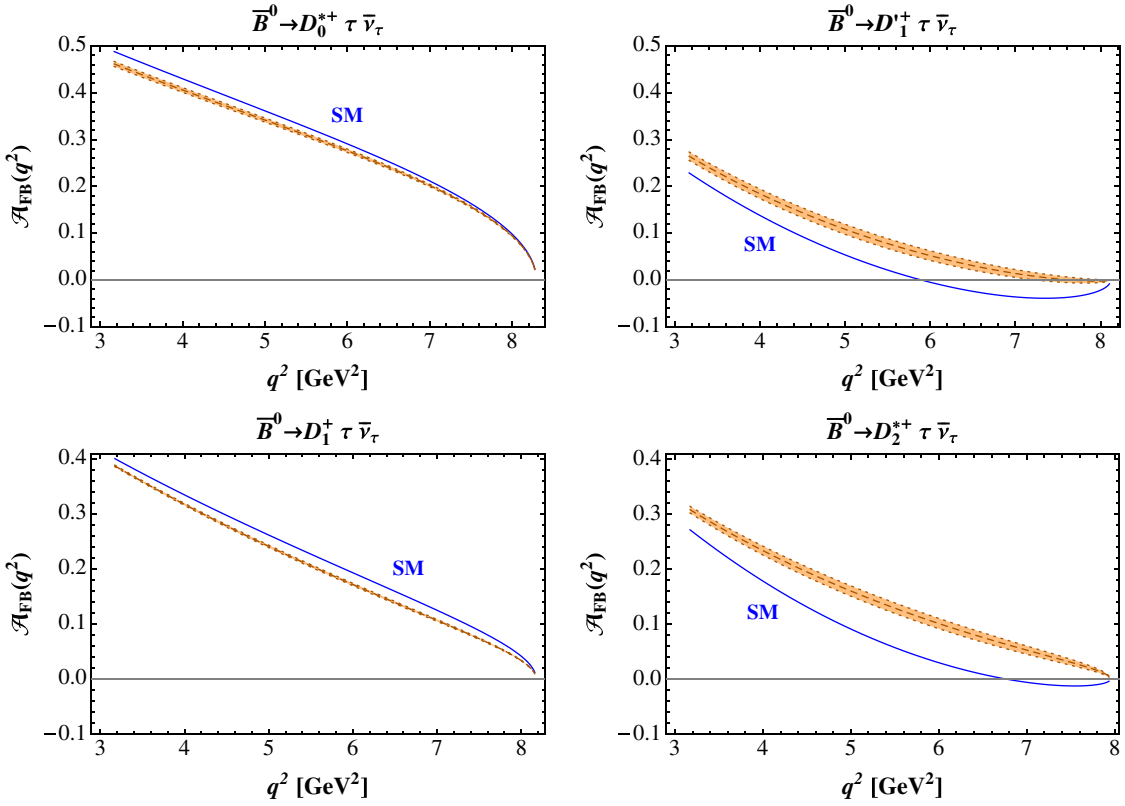

FIG. 10 (color online). Forward-backward asymmetry $\mathcal{A}_{\rm FB}$ for the decays $B \to D_0^* \tau \bar{\nu}_\tau$ (top left), $B \to D_1' \tau \bar{\nu}_\tau$ (top right), $B \to D_1 \tau \bar{\nu}_\tau$ (bottom left) and $B \to D_2^* \tau \bar{\nu}_\tau$ (bottom right) as functions of q^2. The solid (blue) curves are the SM predictions; the dotted (orange) bands are the NP expectations.

moves towards larger values of q^2, and disappears in $B \to D_2^* \tau \bar{\nu}_\tau$ once NP is included.

We close this section by remarking that, while the tensor operator in Eq. (4) does not affect the purely leptonic $B_c \to \tau^- \bar{\nu}_\tau$ mode, it can have an impact on the transitions $B_c \to (\eta_c, J/\psi)\tau^- \bar{\nu}_\tau$ and $\Lambda_b \to \Lambda_c \tau^- \bar{\nu}_\tau$; therefore, sets of other observables can be identified and investigated, with precise correlated deviations from the SM predictions.

V. CONCLUSIONS

The detailed experimental information provided to us on flavor physics shows an astonishing consistency with the SM predictions. The very few tensions identify possible paths to new physics searches. The *BABAR* anomalous enhancement of the ratios $R(D^{(*)}) = \frac{\mathcal{B}(B \to D^{(*)} \tau \bar{\nu}_\tau)}{\mathcal{B}(B \to D^{(*)} \mu \bar{\nu}_\mu)}$ with respect to SM is one of these few cases. The analyses of $R(D^{(*)})$ in specific models also evidentiate the enhancement of the purely leptonic $B \to \tau \bar{\nu}_\tau$ rate, for which data are better compatible with the SM. A mechanism enhancing the semileptonic modes $B \to D^{(*)} \tau \bar{\nu}_\tau$ with respect to $B \to D^{(*)} \mu \bar{\nu}_\mu$, leaving $B \to \tau \bar{\nu}_\tau$ unaffected, can be based on a tensor operator in the effective Hamiltonian. We have bound the relative weight ϵ_T of this operator and studied the impact on several observables, the most sensitive one being the forward-backward asymmetry in $B \to D^* \tau \bar{\nu}_\tau$ with a shift in the position of its zero. If the anomaly in $B \to D^{(*)} \tau \bar{\nu}_\tau$ is due to this NP effect, analogous deviations should be found in B to excited D transitions. The ratios R for these mesons are enhanced with respect to the SM, and the forward-backward asymmetry is a sensitive observable in the channels involving D_1' and D_2^*. These signatures in exclusive semileptonic $b \to c \tau \bar{\nu}_\tau$ modes make the understanding of the role of the new contribution to the effective weak Hamiltonian feasible, a step towards possibly disclosing new interactions through flavor physics measurements.

ACKNOWLEDGMENTS

This work is supported in part by the Italian MIUR Prin 2009.

APPENDIX A: COEFFICIENTS

With the aim of providing information useful for reconstructing the various $B \to D^{(*)}$ matrix elements, we collect here the expressions of the α_s and $1/m_Q$ corrections in Eqs. (21), (22), and (40)–(43) worked out by M. Neubert and by I. Caprini *et al.* in Refs. [28,31]. The functions $L_i(w)$ read as

$$L_1 \simeq 0.72(w-1)\bar{\Lambda}, \qquad L_2 \simeq -0.16(w-1)\bar{\Lambda},$$
$$L_3 \simeq -0.24\bar{\Lambda}, \qquad L_4 \simeq 0.24\bar{\Lambda}, \tag{A1}$$
$$L_5 \simeq -\bar{\Lambda}, \qquad L_6 \simeq -\frac{3.24}{w+1}\bar{\Lambda}.$$

The coefficients C_i are expressed in terms of C_1:

$$\frac{C_1^5}{C_1} = 1 - \frac{4\alpha_s}{3\pi} r_f(w), \qquad \frac{C_2^{(5)}}{C_1} = -\frac{2\alpha_s}{3\pi} H_{(5)}\Big(w, \tfrac{1}{z_m}\Big),$$
$$\frac{C_3^{(5)}}{C_1} = \mp \frac{2\alpha_s}{3\pi} H_{(5)}(w, z_m), \tag{A2}$$

with $z_m = \frac{m_c}{m_b}$ and

$$r_f(w) = \frac{1}{\sqrt{w^2-1}} \log[w + \sqrt{w^2-1}], \tag{A3}$$

$$H_{(5)}(w, z_m) = \frac{z_m(1 - \log z_m \mp z_m)}{1 - 2wz_m + z_m^2} + \frac{z_m}{(1 - 2wz_m + z_m^2)^2} \times [2(w \mp 1)z_m(1 \pm z_m)\log z_m - [(w \pm 1) - 2w(2w \pm 1)z_m + (5w \pm 2w^2 \mp 1)z_m^2 - 2z_m^3]r_f(w)]. \tag{A4}$$

In Eqs. (A2) and (A4), the lower signs refer to the index 5 (corresponding to the axial current). C_1 reads

$$C_1 = \left(\frac{\alpha_s(m_c)}{\alpha_s(\mu)}\right)^{a_{hh}(w)} \left(1 - \frac{\alpha_s(\mu)}{\pi} Z_{hh}(w)\right) \times \left(1 + \frac{\alpha_s(m_c)}{\pi}\left[\log\left(\frac{m_b}{m_c}\right) + Z_{hh}(w) + \frac{2}{3}[f(w) + r_f(w) + g(w)]\right]\right), \tag{A5}$$

with

$$a_{hh}(w) = \frac{8}{27}[w r_f(w) - 1], \tag{A6}$$

$$Z_{hh}(w) = \frac{8}{81}\left(\frac{94}{9} - \pi^2\right)(w-1) - \frac{4}{135}\left(\frac{92}{9} - \pi^2\right)(w-1)^2 + \mathcal{O}((w-1)^3), \tag{A7}$$

$$f(w) = w r_f(w) - 2 - \frac{w}{\sqrt{w^2-1}}[L_2(1 - w_-^2) + (w^2-1)r_f^2(w)], \tag{A8}$$

$$g(w) = \frac{w}{\sqrt{w^2-1}}[L_2(1 - z_m w_-) - L_2(1 - z_m w_+)] - \frac{z_m}{(1 - 2wz_m + z_m^2)}[(w^2-1)r_f(w) + (w - z_m)\log(z_m)], \tag{A9}$$

and $w_\pm = w \pm \sqrt{w^2-1}$. In the numerical analysis, we set the scale $\mu = \sqrt{m_c m_b}$, and investigate the sensitivity to higher-order corrections while varying this scale between $\mu/2$ and 2μ.

APPENDIX B: $B \to D^{**}$ MATRIX ELEMENTS AND DIFFERENTIAL SEMILEPTONIC DECAY RATES

In the infinite heavy-quark mass limit, the $B \to D^{**}$ matrix elements can be defined in terms of two universal $\tau_{1/2}(w)$ and $\tau_{3/2}(w)$ form factors:

$$\langle D_0^*(p')|\bar{c}\gamma_\mu(1-\gamma_5)b|B(p)\rangle = -2\sqrt{m_B m_{D_0^*}}\tau_{1/2}(w)(v - v')_\mu, \tag{B1}$$

$$\langle D_0^*(p')|\bar{c}\sigma_{\mu\nu}(1-\gamma_5)b|B(p)\rangle = 2\sqrt{m_B m_{D_0^*}}\tau_{1/2}(w)[-\epsilon_{\mu\nu\alpha\beta}v^\alpha v'^\beta + i(v_\mu v'_\nu - v_\nu v'_\mu)], \tag{B2}$$

$$\langle D_1'(p',\epsilon)|\bar{c}\gamma_\mu(1-\gamma_5)b|B(p)\rangle = -2\sqrt{m_B m_{D_1'}}\tau_{1/2}(w)[-i\epsilon_{\mu\alpha\beta\sigma}\epsilon^{*\alpha}v^\beta v'^\sigma - (w-1)\epsilon_\mu^* + (\epsilon^*\cdot v)v'_\mu], \tag{B3}$$

$$\langle D_1'(p',\epsilon)|\bar{c}\sigma_{\mu\nu}(1-\gamma_5)b|B(p)\rangle = -2\sqrt{m_B m_{D_1'}}\tau_{1/2}(w)\{-\epsilon_{\mu\nu\alpha\beta}\epsilon^{*\alpha}(v - v')^\beta + i[\epsilon_\mu^*(v - v')_\nu - \epsilon_\nu^*(v - v')_\mu]\}, \tag{B4}$$

$$\langle D_1(p',\epsilon)|\bar{c}\gamma_\mu(1-\gamma_5)b|B(p)\rangle = \frac{\sqrt{m_B m_{D_1}}}{\sqrt{2}}\tau_{3/2}(w)\{i(1+w)\epsilon_{\mu\alpha\beta\sigma}\epsilon^{*\alpha}v^\beta v'^\sigma + (w^2-1)\epsilon_\mu^* + (\epsilon^*\cdot v)[3v_\mu - (w-2)v'_\mu]\}, \tag{B5}$$

$$\langle D_1(p',\epsilon)|\bar{c}\sigma_{\mu\nu}(1-\gamma_5)b|B(p)\rangle = \frac{\sqrt{m_B m_{D_1}}}{\sqrt{2}}\tau_{3/2}(w)\{-(w-1)\epsilon_{\mu\nu\alpha\beta}\epsilon^{*\alpha}(v + v')^\beta + (\epsilon^*\cdot v)\epsilon_{\mu\nu\alpha\beta}v^\alpha v'^\beta + 2\epsilon_{\tau\sigma\alpha\beta}\epsilon^{*\sigma}v^\alpha v'^\beta \times [g_\mu^\tau v_\nu - g_\nu^\tau v_\mu] + i[(1+w)(\epsilon_\nu^*(v - v')_\mu - \epsilon_\mu^*(v - v')_\nu) - 3(\epsilon^*\cdot v)(v_\mu v'_\nu - v_\nu v'_\mu)]\}, \tag{B6}$$

$$\langle D_2^*(p',\epsilon)|\bar{c}\gamma_\mu(1-\gamma_5)b|B(p)\rangle = \sqrt{m_B m_{D_2^*}}\sqrt{3}\tau_{3/2}(w)\{-i\epsilon_{\mu\beta\tau\sigma}(\epsilon^{*\alpha\beta}v_\alpha)v^\tau v'^\sigma + (\epsilon^{*\alpha\beta}v_\alpha)v_\beta v'_\mu - (1+w)(\epsilon_\mu^{*\alpha}v_\alpha)\}, \tag{B7}$$

$$\langle D_2^*(p',\epsilon)|\bar{c}\sigma_{\mu\nu}(1-\gamma_5)b|B(p)\rangle = \sqrt{m_B m_{D_2^*}}\sqrt{3}\tau_{3/2}(w)\{-\epsilon_{\mu\nu\beta\tau}(\epsilon^{*\alpha\beta}v_\alpha)(v + v')^\tau + i(\epsilon^{*\alpha\tau}v_\alpha)[g_\mu^\tau(v + v')_\nu - g_\nu^\tau(v + v')_\mu]\}. \tag{B8}$$

In the previous formulas, we have set $p = m_B v$, $p' = m_{D^{**}} v'$, and $w = v \cdot v'$; ϵ is the polarization vector (tensor) of the spin-1 (spin-2) D^{**} meson.

The results for the SM, NP, and interference contributions to the differential distributions in Eq. (5) are given below for each of the four excited mesons. The relation between the squared momentum transfer q^2 and w is $q^2 = m_B^2 + m_{D^{**}}^2 - 2 m_B m_{D^{**}} w$, with $m_{D^{**}}$ being the mass of the charmed meson produced in the decay. The lepton mass has been taken into account, hence the formulas also hold for τ.

For $B \to D_0^* \ell \bar{\nu}_\ell$:

$$
\begin{aligned}
\frac{d\tilde{\Gamma}}{dq^2}(B \to D_0^* \ell \bar{\nu}_\ell)|_{\rm SM} &= 4 m_B m_{D_0^*} [\tau_{1/2}(w)]^2 (w-1) \left\{ q^2 \left(1 - \frac{m_\ell^2}{q^2}\right) + \left(1 + \frac{2m_\ell^2}{q^2}\right) [(m_B^2 + m_{D_0^*}^2) w - 2 m_B m_{D_0^*}] \right\}, \\
\frac{d\tilde{\Gamma}}{dq^2}(B \to D_0^* \ell \bar{\nu}_\ell)|_{\rm NP} &= 32 |\epsilon_T|^2 m_B m_{D_0^*} [\tau_{1/2}(w)]^2 (w^2-1) \left(1 + \frac{2m_\ell^2}{q^2}\right) (m_B^2 + m_{D_0^*}^2 - 2 m_B m_{D_0^*} w), \\
\frac{d\tilde{\Gamma}}{dq^2}(B \to D_0^* \ell \bar{\nu}_\ell)|_{\rm INT} &= -48\, {\rm Re}(\epsilon_T) m_B m_{D_0^*} [\tau_{1/2}(w)]^2 (w^2-1) m_\ell (m_B - m_{D_0^*}).
\end{aligned}
\tag{B9}
$$

For $B \to D_1' \ell \bar{\nu}_\ell$:

$$
\begin{aligned}
\frac{d\tilde{\Gamma}}{dq^2}(B \to D_1' \ell \bar{\nu}_\ell)|_{\rm SM} &= 4 m_B m_{D_1'} [\tau_{1/2}(w)]^2 (w-1) \left\{ q^2 \left(1 - \frac{m_\ell^2}{q^2}\right)(2w-1) + \left(1 + \frac{2m_\ell^2}{q^2}\right) [(m_B^2 + m_{D_1'}^2) 3w - 2 m_B m_{D_1'} (2w^2+1)] \right\}, \\
\frac{d\tilde{\Gamma}}{dq^2}(B \to D_1' \ell \bar{\nu}_\ell)|_{\rm NP} &= 32 |\epsilon_T|^2 m_B m_{D_1'} [\tau_{1/2}(w)]^2 (w-1) \left(1 + \frac{2m_\ell^2}{q^2}\right) \{ (m_B^2 + m_{D_1'}^2)(5w-1) - 2 m_B m_{D_1'} [4 + w(w-1)] \}, \\
\frac{d\tilde{\Gamma}}{dq^2}(B \to D_1' \ell \bar{\nu}_\ell)|_{\rm INT} &= 48\, {\rm Re}(\epsilon_T) m_B m_{D_1'} [\tau_{1/2}(w)]^2 (w-1) m_\ell [m_B (w-5) + m_{D_1'} (5w-1)].
\end{aligned}
\tag{B10}
$$

For $B \to D_1 \ell \bar{\nu}_\ell$:

$$
\begin{aligned}
\frac{d\tilde{\Gamma}}{dq^2}(B \to D_1 \ell \bar{\nu}_\ell)|_{\rm SM} &= m_B m_{D_1} [\tau_{3/2}(w)]^2 (w-1)(1+w)^2 \left\{ q^2 \left(1 - \frac{m_\ell^2}{q^2}\right)(w-2) \right. \\
&\quad \left. + \left(1 + \frac{2m_\ell^2}{q^2}\right) [(m_B^2 + m_{D_1}^2) 3w - 2 m_B m_{D_1} (w^2+2)] \right\}, \\
\frac{d\tilde{\Gamma}}{dq^2}(B \to D_1 \ell \bar{\nu}_\ell)|_{\rm NP} &= 16 |\epsilon_T|^2 m_B m_{D_1} [\tau_{3/2}(w)]^2 (w-1)(1+w)^2 \left(1 + \frac{2m_\ell^2}{q^2}\right) \{ [(m_B^2 + m_{D_1}^2)(2w-1) - 2 m_B m_{D_1} (w^2 - w + 1)] \}, \\
\frac{d\tilde{\Gamma}}{dq^2}(B \to D_1 \ell \bar{\nu}_\ell)|_{\rm INT} &= 24\, {\rm Re}(\epsilon_T) m_B m_{D_1} [\tau_{3/2}(w)]^2 (w-1)(1+w)^2 m_\ell [m_B (w-2) + m_{D_1} (2w-1)].
\end{aligned}
\tag{B11}
$$

For $B \to D_2^* \ell \bar{\nu}_\ell$:

$$
\begin{aligned}
\frac{d\tilde{\Gamma}}{dq^2}(B \to D_2^* \ell \bar{\nu}_\ell)|_{\rm SM} &= m_B m_{D_2^*} [\tau_{3/2}(w)]^2 (w-1)(1+w)^2 \left\{ q^2 \left(1 - \frac{m_\ell^2}{q^2}\right)(3w+2) \right. \\
&\quad \left. + \left(1 + \frac{2m_\ell^2}{q^2}\right) [(m_B^2 + m_{D_2^*}^2) 5w - 2 m_B m_{D_2^*} (3w^2+2)] \right\}, \\
\frac{d\tilde{\Gamma}}{dq^2}(B \to D_2^* \ell \bar{\nu}_\ell)|_{\rm NP} &= 16 |\epsilon_T|^2 m_B m_{D_2^*} [\tau_{3/2}(w)]^2 (w-1)(1+w)^2 \left(1 + \frac{2m_\ell^2}{q^2}\right) \{ [(m_B^2 + m_{D_2^*}^2)(1+4w) - 2 m_B m_{D_2^*} (3 + w + w^2)] \}, \\
\frac{d\tilde{\Gamma}}{dq^2}(B \to D_2^* \ell \bar{\nu}_\ell)|_{\rm INT} &= -24\, {\rm Re}(\epsilon_T) m_B m_{D_2^*} [\tau_{3/2}(w)]^2 (w-1)(1+w)^2 m_\ell [m_B (4+w) - m_{D_2^*} (1+4w)].
\end{aligned}
\tag{B12}
$$

The differential decay rates are obtained by multiplying the above functions by the coefficient $C(q^2)$ in Eq. (6).

[1] J. P. Lees *et al.* (*BABAR* Collaboration), Phys. Rev. Lett. **109**, 101802 (2012).
[2] S. Fajfer, J. F. Kamenik, and I. Nisandzic, Phys. Rev. D **85**, 094025 (2012).
[3] S. Fajfer, J. F. Kamenik, I. Nisandzic, and J. Zupan, Phys. Rev. Lett. **109**, 161801 (2012).
[4] A. Crivellin, C. Greub, and A. Kokulu, Phys. Rev. D **86**, 054014 (2012).
[5] A. Datta, M. Duraisamy, and D. Ghosh, Phys. Rev. D **86**, 034027 (2012).
[6] D. Becirevic, N. Kosnik, and A. Tayduganov, Phys. Lett. B **716**, 208 (2012).
[7] A. Celis, M. Jung, X.-Q. Li, and A. Pich, J. High Energy Phys. 01 (2013) 054.
[8] D. Choudhury, D. K. Ghosh, and A. Kundu, Phys. Rev. D **86**, 114037 (2012).
[9] M. Tanaka and R. Watanabe, Phys. Rev. D **87**, 034028 (2013).
[10] J. Laiho, E. Lunghi, and R. S. Van de Water, Phys. Rev. D **81**, 034503 (2010), and the average quoted in http://latticeaverages.org/.
[11] M. Bona *et al.* (UTfit Collaboration), Phys. Lett. B **687**, 61 (2010).
[12] A. Lenz, U. Nierste, J. Charles, S. Descotes-Genon, A. Jantsch, C. Kaufhold, H. Lacker, S. Monteil, V. Niess, and S. T'Jampens, Phys. Rev. D **83**, 036004 (2011).
[13] B. Aubert *et al.* (*BABAR* Collaboration), Phys. Rev. D **77**, 011107 (2008).
[14] B. Aubert *et al.* (*BABAR* Collaboration), Phys. Rev. D **81**, 051101 (2010).
[15] K. Ikado *et al.* (Belle Collaboration), Phys. Rev. Lett. **97**, 251802 (2006).
[16] K. Hara *et al.* (Belle Collaboration), Phys. Rev. D **82**, 071101 (2010).
[17] J. L. Rosner and S. Stone, arXiv:1201.2401.
[18] I. Adachi *et al.* (Belle Collaboration), arXiv:1208.4678.
[19] J. P. Lees *et al.* (*BABAR* Collaboration), arXiv:1207.0698.
[20] H. Georgi and S. L. Glashow, Phys. Rev. Lett. **32**, 438 (1974); S. Chakdar, T. Li, S. Nandi, and S. K. Rai, Phys. Lett. B **718**, 121 (2012).
[21] J. C. Pati and A. Salam, Phys. Rev. D **10**, 275 (1974); **11**, 703(E) (1975).
[22] B. Schrempp and F. Schrempp, Phys. Lett. **153B**, 101 (1985); W. Buchmuller, R. Ruckl, and D. Wyler, Phys. Lett. B **191**, 442 (1987); **448**, 320(E) (1999).
[23] J. L. Hewett and T. G. Rizzo, Phys. Rep. **183**, 193 (1989).
[24] S. Dimopoulos and L. Susskind, Nucl. Phys. **B155**, 237 (1979); S. Dimopoulos, Nucl. Phys. **B168**, 69 (1980); E. Eichten and K. D. Lane, Phys. Lett. **B90**, 125 (1980).
[25] CMS Collaboration, Report No. CMS-PAS-EXO-12-002.
[26] S. Rolli and M. Tanabashi, review *Leptoquarks* in Ref. [41].
[27] N. Isgur and M. B. Wise, Phys. Lett. B **237**, 527 (1990).
[28] M. Neubert, Phys. Rep. **245**, 259 (1994).
[29] F. De Fazio, in *At the Frontier of Particle Physics*, Handbook of QCD, edited by M. Shifman (World Scientific, Singapore, 2001), Vol. 4, p. 1671; A. V. Manohar and M. B. Wise, Cambridge Monogr. Part. Phys., Nucl. Phys., Cosmol. **10**, 1 (2000).
[30] B. Aubert *et al.* (*BABAR* Collaboration), Phys. Rev. Lett. **104**, 011802 (2010).
[31] I. Caprini, L. Lellouch, and M. Neubert, Nucl. Phys. **B530**, 153 (1998).
[32] W. Dungel *et al.* (Belle Collaboration), Phys. Rev. D **82**, 112007 (2010).
[33] J. P. Lees *et al.* (*BABAR* Collaboration), arXiv:1303.0571.
[34] A comprehensive analysis of the open charm meson spectrum can be found in P. Colangelo, F. De Fazio, F. Giannuzzi, and S. Nicotri, Phys. Rev. D **86**, 054024 (2012).
[35] D. Becirevic, A. Le Yaouanc, L. Oliver, J.-C. Raynal, P. Roudeau, and J. Serrano, Phys. Rev. D **87**, 054007 (2013).
[36] P. Colangelo, G. Nardulli, and N. Paver, Phys. Lett. B **293**, 207 (1992).
[37] P. Colangelo, F. De Fazio, and N. Paver, Nucl. Phys. B, Proc. Suppl. **75**, 83 (1999).
[38] P. Colangelo, F. De Fazio, and N. Paver, Phys. Rev. D **58**, 116005 (1998).
[39] V. Morenas, A. Le Yaouanc, L. Oliver, O. Pene, and J. C. Raynal, Phys. Rev. D **56**, 5668 (1997).
[40] B. Blossier, M. Wagner, and O. Pène (European Twisted Mass Collaboration), J. High Energy Phys. 06 (2009) 022.
[41] J. Beringer *et al.* (Particle Data Group), Phys. Rev. D **86**, 010001 (2012).